J. Math. Biol. (1997) 36: 41–63

Journal of
Mathematical
Biology

Modelling of the baroreflex-feedback mechanism with time-delay

Johnny T. Ottesen

IMFUFA, Roskilde University, Postbox 260, DK-4000 Roskilde, Denmark
E-mail: Johnny@mmf.ruc.dk

Received 1 June 1996; received in revised form 20 November 1996

Abstract. The cardiovascular system is considered. A direct modelling of the non-linear baroreflex-feedback mechanism, including time-delay, is developed based on physiological theory and empirical facts. The feedback model is then evaluated on an expanded, but simple, non-pulsatile Windkessel model of the cardiovascular system. The stability of the entire model is analyzed and the effect of the value of the time-delay is investigated and discussed. The time-delay may cause oscillations. A finite number of stability switches may occur dependent on the value of the time-delay. The location of these stability switches turns out to be sensitive to the value of the parameters in the model. We suggest a simple experiment to determine whether or not the time-delay is responsible for the 10 second Mayer waves. Data from an ergometer bicycle test is used for evaluation of the model.

Key words: Cardiovascular system – Nonlinear baroreflex-feedback – Time-delay – Stability analysis

1 Introduction

We consider the systemic part of the cardiovascular system, consisting of the left ventricle, the arteries, the capillaries, the veins, and the right ventricle, together with the baroreflex-feedback mechanism.

The mathematical modelling of this system, without feedback, can be approached in several ways. One may derive partial differential equations, describing the blood as a Newtonian fluid, for this approach see for example Lighthill (1975), Peskin (1976), Pedley (1980), Berger (1993) and Olufsen and Ottesen (1995). Rather than this, we make the model as rough as possible, focusing on simple and well-established physical principles, and make as many simplifying physical assumptions as possible. Hereby, a system of ordinary differential equations with only a few variables is obtained, for this approach see Warner (1958), Grodins (1959), Warner and Cox (1962), Warner

(1962), Grodins (1963), Milhorn (1966), Taylor (1978), Noordergraaf (1978), Ursino (1995) and Cavalcanti et al. (1995). This part of the modelling is based on theoretical physics (Sect. 2). Having a model of the uncontrolled cardiovascular system (that is, excluding feedback mechanisms) we extend the model, by adding an explicit modelling of the baroreflex-feedback mechanism, describing how the heart rate is regulated, called the chronotropic effect, and how the contractility of the ventricle is regulated, called the inotropic effect. There have been several attempts to model the accumulated effect of the baroreflex-feedback mechanism as a regulator by standard methods known from control theory. Noldus (1976) used optimal control based on a principle of minimal energy consumption whereas Ono et al. (1982) and Kappel and Peer (1993) used optimal control based on a principle of minimal deviation from a set-point. None of these are based on well-established physiological knowledge. Rideout (1991) and Tham (1988) used principles from linear control theory, even though the feedback is not linear. We prefer to model the feedback mechanism directly. Our approach is based on well-established physiological theory and empirical facts (Sects. 3–4). This feedback mechanism introduces some non-linearity in the model and includes a time-delay. Special attention is paid to the effect of the time-delay.

When such a feedback model is produced, we apply methods from non-linear analysis, which are useful in this connection. The various possible scenarios, caused by different values of the time-delay, are discussed together with a possible relation to the 10 second Mayer waves (Sect. 5). Moreover an ergometer bicycle test is simulated and compared to real data (Sect. 6). However, it is not possible to solve all equations analytically, and we therefore include numerical considerations.

Finally a discussion and an outlook is given (Sect. 7) and the nominal values of the parameters used are listed (Appendix).

One may model the pulmonary part of the cardiovascular system in a similar way as the systemic part. A model of the entire cardiovascular system does not separate into two uncoupled submodels, even when pressure independent stroke volumes are assumed, because of conservation of the total blood volume. However, such a model includes a submodel of the systemic part of the cardiovascular system, which is independent of the rest of the system. Therefore, an analysis of the systemic part of the cardiovascular system is sufficient for our considerations.

2 Mathematical model of the uncontrolled non-pulsatile system

First we consider the systemic part of the cardiovascular system, consisting of the left ventricle, the arteries, the capillaries, the veins, and the right ventricle, without feedback mechanisms. Later on we add a model of the baroreflex-feedback mechanism.

Since our goal is to analyze the baroreflex-feedback mechanism, the model of the uncontrolled system must be as simple as possible, but it still has to

catch certain principal characteristics of the system. With this we can handle the feedback model and understand the basic mechanism of the real system being modelled.

We include the left ventricle in the model only to describe the inflow to the aorta. Therefore, we describe it simply as a source term, i.e. the inflow is a given function of time. This function is chosen to agree with measurements and depends on heart rate and stroke volume (or contractility).

The arteries are considered as a compartment characterized by a compliance. The pressure in the arterial compartment is determined by the difference between inflow to and outflow from the compartment, see Fig. 1.

From the arteries there is an outflow, through the capillaries, to the venous part. Since the major drop in pressure occurs over the capillaries, Guyton (1981), they are characterized by a resistance to the flow. Hence, the flow through the capillaries is determined by the difference in pressure between the arterial and the venous part.

Analogous to the arteries, the veins are considered as a compliant compartment.

The flow out of the veins is into the right ventricle, ignoring the right atrium. The ventricle is simply described as a sink, characterized by a resistance to the flow out.

The above idealizations, lumping the systems into compartments, as shown on Fig. 1, are rough in some respects, e.g. one looses information about spatial properties. However, it turns out that the model is adequate for the following analysis of the baroreflex-feedback mechanism.

In what follows we consider the blood as an incompressible Newtonian fluid and ignore the fluid exchange between the blood circulation and the interstitial fluid space.

Following basic conservation laws of physics, see for example Grodins (1959) and Noordergraaf (1978), we arrive at a system of differential equations for the uncontrolled non-pulsatile cardiovascular system

$$\begin{pmatrix} \dot{P_a}(t) \\ P_v(t) \end{pmatrix} = \begin{pmatrix} -\dfrac{1}{c_a R} & \dfrac{1}{c_a R} \\ \dfrac{1}{c_v R} & -\dfrac{1}{c_v}\left(\dfrac{1}{r}+\dfrac{1}{R}\right) \end{pmatrix} \begin{pmatrix} P_a(t) \\ P_v(t) \end{pmatrix} + \frac{1}{c_a} H V_{\text{str}} \begin{pmatrix} 1 \\ 0 \end{pmatrix} \tag{1}$$

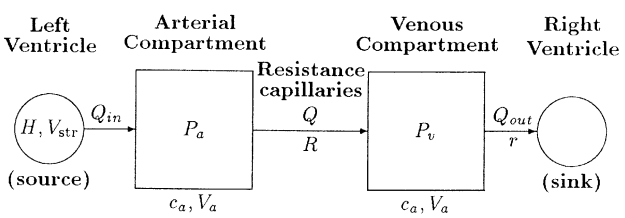

Fig. 1. A lumped uncontrolled model of the cardiovascular system

where $P_a(t)$ and $P_v(t)$ denote the arterial and venous mean pressure respectively (the average is taken over a heart cycle), c_a and c_v are the compliances of the arterial and the venous compartments, respectively, R and r are the resistances to flow through the systemic capillaries and the flow out of the venous compartment (i.e. the right ventricle is considered as a sink), respectively, and H and V_{str} are the heart rate and the stroke volume, respectively. The determinant is $\frac{1}{c_a R}\frac{1}{c_v r} \neq 0$ and it easily follows that $HV_{\text{str}} r\binom{1+R/r}{1}$ is a uniquely determined stationary point. Since it is uniquely determined by the heart rate, the stroke volume and the two resistances to flow, the stationary point may be used to estimate r and R independently of c_a and c_v. The characteristic roots are both real and negative

$$\lambda_{\pm} = -\frac{1}{2}\left(\frac{1}{R}\left(\frac{1}{c_a}+\frac{1}{c_v}\right)+\frac{1}{c_v r}\right) \pm \sqrt{\frac{1}{4}\left(\frac{1}{R}\left(\frac{1}{c_a}+\frac{1}{c_v}\right)+\frac{1}{c_v r}\right)^2 - \frac{1}{c_a R}\frac{1}{c_v r}} \tag{2}$$

Thus, the system is asymptotically stable. The transient, which is determined by the characteristic roots, depends on the resistances, as well as the compliances. With the nominal values for the parameters, given in appendix, $\lambda_+ = -0.0283$ and $\lambda_- = -0.615\ \text{sec}^{-1}$, and the corresponding eigenvectors are $(-0.72,\ -0.69)$ and $(-1.00, 0.003)$, respectively. Then the characteristic times of the system become 35.4 and 1.63 seconds. So the arterial part shows a fast transient whereas the venous part shows a relative slow transient.

It follows that the system is completely linear controllable and observable (see for example Russel (1979) or Lee and Markus(1967)). However investigations (see Sect. 4) show that the physiological control mechanism is non-linear. Therefore linear control theory does not suffice and non-linear control theory is needed. Alternatively one may turn the system into a close-loop control system, by modelling the non-linear feedback mechanism $H = H(P_a)$ and $V_{\text{str}} = V_{\text{str}}(P_a)$ directly. Indeed this is the approach to be followed.

3 Control mechanisms of the cardiovascular system

In this section we briefly discuss the control mechanisms of the cardiovascular system and, in particular, the baroreflex-feedback mechanism.

Blood pressure is controlled by a large number of control mechanisms. The entire control system is very complex and the individual parts normally interact in a complicated manner, Guyton (1981). However, the system may be divided into at least two categories, autoregulation, which is due to the hemodynamic properties of the cardiovascular system, and nervous control. The baroreflex-feedback mechanism, which we consider here, belongs to the latter category, and is a short-term blood pressure control mechanism.

The baroreceptors are tension-sensitive nerve fiber endings located at various places in the circulatory system. It is believed that those located in the aortic arch and in the carotid sinus are the most important ones, see Fig. 2. The baroreceptors sense the local pressure and cause a change in frequency in

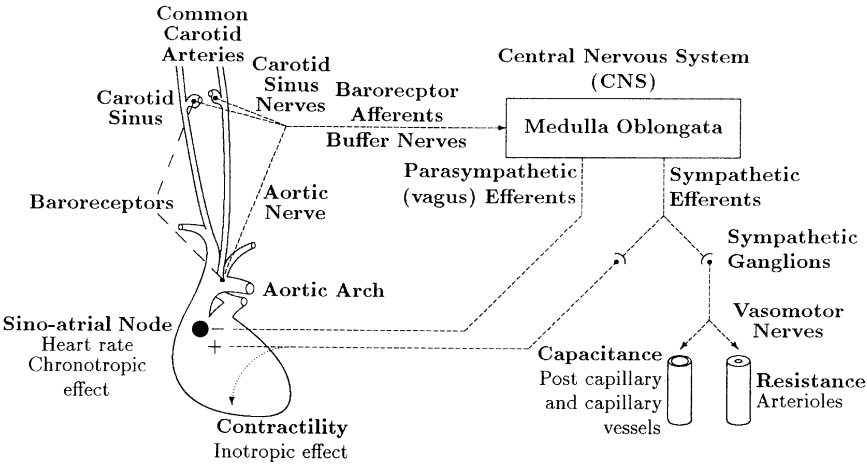

Fig. 2. The baroreceptor feedback system

nerve activity. This nerve activity is transmitted, through the afferent nerve fibers, to the vagal center and the vasomotor center at medulla oblongata in the central nervous system. The heart rate, the contractility and then the stroke volume of the ventricles, the peripheral resistances, and the arterial and venous capacities and unstressed volumes are controlled by the central nervous system, through the sympathetic and the parasympathetic nerve activity (see Fig. 2). All these control mechanisms serve to control the arterial pressure, i.e. to steer the pressure toward some "normal" set–point. Here, and throughout this paper, the term set-point denote a steady-state, determined by physiological parameters of the model, toward which the pressure converges.

In the following we will only consider the system consisting of the arterial pressure, the baroreceptors, the nerve fibers going to the central nervous system, the central nervous system, the sympathetic and the parasympathetic nerve fibers going to the heart, the change in heart rate caused by the activity in these nerves (through the hormonal transmitters, norepinephrine and acetylcholine) and in stroke volume (through contractility) caused by the activity in the sympathetic nerves. Moreover, we reserve the phrase "the baroreflex-feedback mechanism" to mean exactly this subsystem. In Fig. 3 we have sketched the cardiovascular system, as modeled earlier, together with this baroreflex-feedback mechanism.

To model the chronotropic effect of the baroreflex-feedback mechanism explicitly, we divide this system into two parts. The first part is described by the firing rates (nerve activity) of the nerve fibers, called the tones, at the nerve fiber endings going to the heart. The tones are functions of the arterial blood pressure. The second part is described by the change in heart rate as a function of the sympathetic and the parasympathetic tones. Measurements show that there is a time-delay of the order of 10 seconds for the peak response (maximal

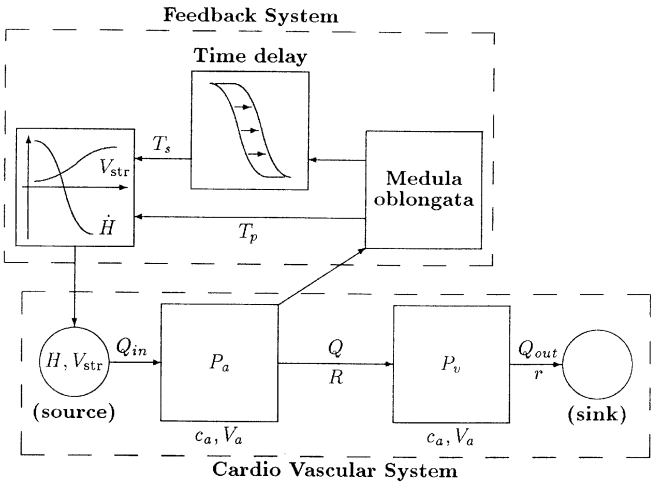

Fig. 3. The controlled cardiovascular system

effect) to appear in the sympathetic nervous system and of the order of less than 1 second in the parasympathetic nervous system, see Guyton and Harris (1951), Warner (1958), Warner and Russel (1969), Korner (1971) Milhorn (1966) and Borst and Karemaker (1983). Hence the actual time-delay, assuming a simple one, is, in accordance with the measurements, a factor 10 times larger in the sympathetic system than in the parasympathetic system. This is because of the quick hydrolysis of the acetylcholine released by parasympathetic stimulation as compared with the slow reuptake and washout of the sympathetically released norepinephrine at the heart. Therefore, we include the time-delay in the sympathetic nervous system and ignore that of the parasympathetic nervous system. In the literature Warner (1958) and Warner and Russel (1969) estimate the time-delay to be in the range 2 to 4 seconds, Cavalcanti et al. (1995) use $\tau = 2.5$ seconds, Rideout (1991) has $\tau \approx 3$ seconds (in Rideout it is an average value of a continuous delay), and Guyton and Harris (1951) estimate it to be 13 seconds. Each of the above two parts is fairly well-known qualitatively, but quantitatively they are only roughly known.

Less is known about how the inotropic effect of the baroreflex-feedback mechanism works. But it seems that the stroke volume increases slightly with the mean arterial pressure, through the sympathetic nerve system, in the physiological range under consideration.

4 Mathematical model of the baroreflex-feedback mechanism

In this section a mathematical model for the baroreflex-feedback mechanism, described in Sect. 3, will be developed.

First we consider the chronotropic effect. As mentioned earlier we divide this feedback system into two parts.

The model describing the first part of this feedback mechanism is based on measurements of the sympathetic and the parasympathetic tones as functions of the mean arterial pressure, see Korner (1971) and references therein. Graphs of the qualitative behavior of these functions are both sigmoidal in shape.

It follows that the sympathetic tone T_s and the parasympathetic tone T_p are decreasing and increasing as functions of the mean arterial pressure, respectively, i.e.

$$T_s = g_s(P_a^\tau), \qquad g_s'(P_a^\tau) < 0\,,$$

$$T_p = g_p(P_a), \qquad g_p'(P_a) > 0$$

and

$$g_s \approx 1 \quad \text{for } P_a^\tau \text{ small}, \qquad g_s \approx 0 \quad \text{for } P_a^\tau \text{ large}\,,$$
$$g_p \approx 0 \quad \text{for } P_a \text{ small}, \qquad g_p \approx 1 \quad \text{for } P_a \text{ large}$$

where P_a^τ and P_a denote the mean arterial pressure with and without time-delay, respectively, τ characterizes the time-delay. Otherwise g_s and g_p are unspecified functions.

Example. As an ad hoc model one may choose

$$g_s(P_a^\tau) = \frac{1}{1 + \left(\dfrac{P_a^\tau}{\alpha_s}\right)^{\beta_s}}$$

and

$$g_p(P_a) = \frac{1}{1 + \left(\dfrac{P_a}{\alpha_p}\right)^{-\beta_p}}$$

where the parameters α_s, α_p, β_s and β_p are all positive and characterize the location and steepness of the curves, i.e.

$$g_s = \frac{1}{2} \quad \text{for } P_a^\tau = \alpha_s, \qquad g_p = \frac{1}{2} \quad \text{for } P_a = \alpha_p\,,$$

$$g_s' = -\frac{\beta_s}{4\alpha_s} \quad \text{for } P_a^\tau = \alpha_s, \qquad g_p' = \frac{\beta_p}{4\alpha_s} \quad \text{for } P_a = \alpha_p\,.$$

Nominal values are $\alpha_s = \alpha_p = 93$ mmHg and $\beta_s = \beta_p = 7$ for a person at rest.

We emphasize that the phrase "mean pressure" in the pulsatile case may not mean the ordinary average value over a cycle, as in the non-pulsatile case, but rather a weighted average.

The model describing the second part of the chronotropic effect of the baroreflex-feedback mechanism is based on measurements of the change in heart rate as a function the tones, which may be found in a paper by Levy and Zieske (1969). From these measurements one may conclude that the change in heart rate is an increasing function of the sympathetic tone and a decreasing function of the parasympathetic tone, and furthermore an increase in the

parasympathetic tone will reduce the effect of the sympathetic tone on the change in heart rate. We write

$$\dot{H}(t) = h(T_s, T_p)$$

where

$$\frac{\partial h}{\partial T_s}(T_s, T_p) > 0 \quad \text{and} \quad \frac{\partial h}{\partial T_p}(T_s, T_p) < 0$$

and

$$\frac{\partial h}{\partial T_s}(T_s, T_p) \text{ decreases with respect to } T_p$$

Moreover, $h = \dot{H} < 0$ for $T_s \approx 0$ and $T_p \approx 1$, corresponding to high pressures, and $h = \dot{H} > 0$ for $T_s \approx 1$ and $T_p \approx 0$, corresponding to low pressures. Otherwise h is unspecified.

Example. As an ad hoc model one may choose

$$\dot{H}(t) = \frac{\alpha_H T_s}{1 + \gamma_H T_p} - \beta_H T_p$$

where the parameters α_H and β_H express the strength with which the sympathetic tone and the parasympathetic tone, respectively, influence the change in heart rate, and γ_H express the damping from the parasympathetic nervous system on the strength with which the sympathetic nervous system influence the change in heart rate. All parameters are positive. Notice that, $\dot{H} \approx -\beta_H < 0$ for high pressure and that $\dot{H} \approx \alpha_H > 0$ for low pressure. Nominal values are $\alpha_H = 0.84 \text{ sec}^{-2}$ and $\beta_H = 1.17 \text{ sec}^{-2}$. These values reflect the fact that at normal heart rate, the parasympathetic stimulation is more dominant than the sympathetic stimulation, so the normal heart rate is lower than the intrinsic rate of the denervated heart. It turns out that h is little sensitive to γ_H, and one may choose $\gamma_H = 0$ to simplify the analysis.

Putting the above two submodels together in one model of the chronotropic effect of the baroreflex-feedback mechanism we obtain a non-linear differential equation with time-delay

$$\dot{H}(t) = f(P_a(t), P_a(t - \tau))$$

where we use that the time-delay in the non-pulsatile case is given by $P_a^\tau(t) = P_a(t - \tau)$ and $f = h \circ g$. Hence, $\dot{H}$ is negative for high pressures and $\dot{H}$ is positive for low pressures. Furthermore, $\dot{H}$ is monotonic decreasing in each variable, i.e. $\partial f / \partial P_a < 0$ and $\partial f / \partial P_a^\tau < 0$.

Combining the two ad hoc submodels above it follows that the physiological parameters $\alpha_H, \beta_H, \alpha_s, \beta_s, \alpha_p$, and β_p determine the set-point for the steady state, see Sect. 5. This function $f(P_a, P_a^\tau)$ for the nominal value of the parameters is shown in Fig. 4.

The inotropic effect of the baroreflex-feedback mechanism is less known than the chronotropic effect. From Suga et al. (1974) and Wesseling et al. (1982) it follows that the contractility increases when P_a decreases, but at the

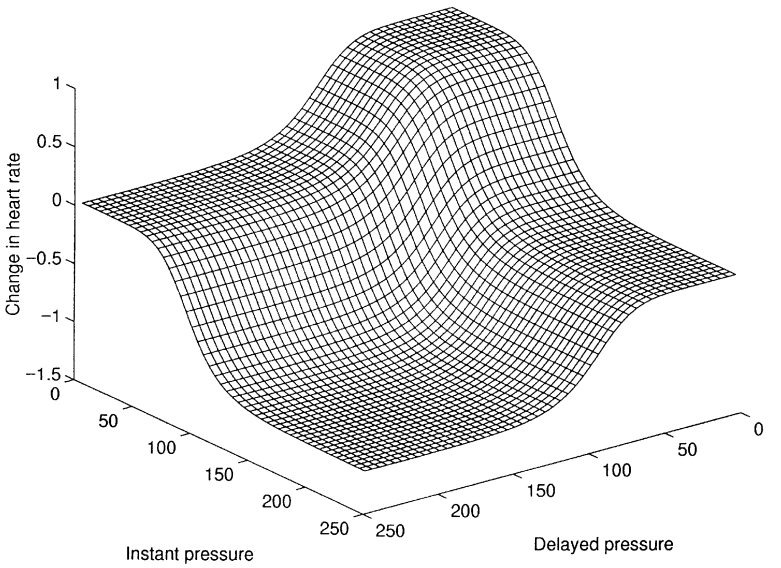

Fig. 4. The change in heart rate as a function of the delayed pressure P_a^τ and the instant pressure P_a

same time t_s decreases. Following Allison et al. (1969), Suga et al. (1976) and Cavalcanti et al. (1995), V_{str} is approximately constant in the physiological range under consideration and is increasing with P_a for low pressure. However, we emphasize that this may vary depending on the fitness of the person (for an athlete the contractility increase first and the heart rate secondly when exercising). It turns out that the following analysis does not change qualitatively when V_{str} is constant or variate, as long as P_a is in the physiological range under consideration. But in case of variable V_{str} the analysis becomes more technical. For simplicity we keep V_{str} fixed in what follows. Furthermore, it is not in general clear how the "set-point" for V_{str} behaves qualitatively when the system is disturbed, but in some situations it is known. In agreement with this knowledge we assume that this "set-point" changes similar to how the set-point for the heart rate changes. In fact, we will only consider the case where the peripheral resistance increases exponentially, corresponding to a change from rest to exercise (a short term submaximal workload). In this case it is expected that the set-points behave similarly. We return to this question in Sect. 6.

We are now able to analyze the model of the closed-loop control system of the cardiovascular system, which we will call the baroreflex-feedback model, given by the model for the uncontrolled non-pulsatile cardiovascular system described by equation (15), together with the model of the baroreflex-feedback mechanism just derived.

5 Analysis of the baroreflex-feedback model

5.1 Existence and uniqueness of an equilibrium

In this section we will analyse the baroreflex-feedback model given by the following system of non-linear differential equation with time-delay. From above it follows that

$$\begin{aligned}
\dot{P}_a(t) &= -\frac{1}{c_a R} P_a(t) + \frac{1}{c_a R} P_v(t) + \frac{1}{c_a} V_{\text{str}}(P_a^\tau(t)) H(t) \\
\dot{P}_v(t) &= \frac{1}{c_v R} P_a(t) - \left(\frac{1}{c_v R} + \frac{1}{c_v r} \right) P_v(t) \\
\dot{H}(t) &= f(P_a(t), P_a(t-\tau))
\end{aligned} \tag{3}$$

Notice that the non-linearity and the time-delay only appear through the feedback equations when V_{str} is assumed constant. Due to a well-known theorem (see for example El'sgol'ts and Norkin (1973)), continuity of f, g and ϕ, where ϕ is the initial condition in $[t_0 - \tau, t_0]$, guarantee existence of solutions to equation (3). Moreover, if the right hand side of equation (3) is Lipschitz continuous, uniqueness also follows. However, these general results are not needed here.

In the following we make physiologically realistic assumptions on f, which are justified in Sect. 4,

$$\begin{aligned}
&f > 0 \quad \text{for } P_a \text{ and } P_a^\tau \text{ small}, \\
&f < 0 \quad \text{for } P_a \text{ and } P_a^\tau \text{ large}, \\
&f \text{ is differentiable, and} \\
&\frac{\partial f}{\partial P_a} < 0 \quad \text{and} \quad \frac{\partial f}{\partial P_a^\tau} < 0
\end{aligned} \tag{4}$$

We notice that when $P_a^\tau = P_a$ these assumptions imply that

$$\begin{aligned}
&f > 0 \quad \text{for } P_a \text{ small}, \\
&f < 0 \quad \text{for } P_a \text{ large, and} \\
&f \text{ is monotonic decreasing and continuous}
\end{aligned} \tag{5}$$

In fact, it is the weaker assumptions (5) that we are going to use, when we investigate the questions of existence and uniqueness of an equilibrium.

Theorem 1. *Under the assumption* (5) *the system given by equation* (3) *has a uniquely determined equilibrium.*

Proof. We first notice that if the system is in an equilibrium, then $P_a^\tau = P_a$. In this case we simply write $\dot{H} = f(P_a)$. By the assumptions, it follows that there exists a uniquely determined "set–point" value $P_a = P_0$, such that $f(P_0) = 0$.

Then the system, given by equation (3), uniquely determines P_v and H as

$$P_v(t) = \frac{1}{1 + \dfrac{R}{r}} P_0 \tag{6}$$

and

$$H(t) = \frac{1}{RV_{\text{str}}(P_0)} \frac{1}{1 + \dfrac{r}{R}} P_0 \tag{7}$$

where at equilibrium $V_{\text{str}}(P_a(t)) = V_{\text{str}}(P_0)$. Hereby, the existence and uniqueness of an equilibrium is shown. □

We emphasize that the proof for existence and uniqueness of an equilibrium only uses assumption (5) and the fact that the arterial pressure determines all the other state variables uniquely at the equilibrium.

Notice, that it follows that the ratio between the mean arterial pressure and the mean venous pressure is given by $1 + R/r \approx 16.4$ and that the ratio between the mean arterial pressure and the inflow is given by $R(1 + r/R) \approx 1.12$ mmHg sec/ml at the equilibrium, i.e. in steady state.

Example. Continuing with the examples given in Sect. 4 the so-called set-point becomes

$$P_0 = \alpha_0 \left(\frac{\alpha_H}{\beta_H} \right)^{1/\beta_0}$$

for $\alpha_0 = \alpha_s = \alpha_p$ and $\beta_0 = \beta_s = \beta_p$ as in the case of the nominal values given in appendix. The physiological estimated range of $(\alpha_H/\beta_H)^{1/\beta_0}$ then becomes 0.8 to 1.2 and $P_0 \approx \alpha_0$.

5.2 Stability of the equilibrium

We will now investigate the stability of the equilibrium and how it depends on the value of the time-delay. But as mentioned earlier, the analysis is quite technical due to the number of uncertain parameters when linearizing equation (3). However, it turns out that the qualitative behavior of the system agrees with that in which V_{str} is assumed constant. So for simplicity we will consider this case here and return to the full feedback system in the discussion and when simulating data, obtained by an ergometer bicycle test, in Sect. 6. Hence we consider the feedback system

$$\begin{aligned}
\dot{P}_a(t) &= -\frac{1}{c_a R} P_a(t) + \frac{1}{c_a R} P_v(t) + \frac{1}{c_a} V_{\text{str}} H(t) \\
\dot{P}_v(t) &= \frac{1}{c_v R} P_a(t) - \left(\frac{1}{c_v R} + \frac{1}{c_v r} \right) P_v(t) \\
\dot{H}(t) &= f(P_a(t), P_a(t - \tau))
\end{aligned} \tag{8}$$

with the unique equilibrium

$$P_a = P_0, \qquad P_v(t) = \frac{1}{1+\frac{R}{r}} P_0 \quad \text{and} \quad H(t) = \frac{1}{RV_{\text{str}}} \frac{1}{1+\frac{r}{R}} P_0$$

Before examining the question of stability of the equilibrium, it is appropriate to transform the system into dimensionless form. Consider the transformation $(P_a, P_v, H, t) \to (x_a, x_v, x_h, s)$, given by

$$\begin{aligned} P_a &= x_a P_0 \\ P_v &= x_v P_0 \\ H &= x_h \frac{c_a P_0}{V_{\text{str}} t_0} \\ t &= s t_0 \end{aligned}$$

where $P_0 (\approx 100\ \text{mmHg})$ is the arterial equilibrium pressure and $t_0 = c_a R$ $(\approx 1.6\ \text{sec})$ is a characteristic time. With this the number of parameters reduces, and equation (3) transforms into

$$\begin{aligned} \dot{x}_a &= -x_a + x_v + x_h \\ \dot{x}_v &= \alpha x_a - \beta x_v \\ \dot{x}_h &= \tilde{f}(x_a, x_a^\tau) \end{aligned} \tag{9}$$

where $\alpha = c_a/c_v \approx 3.0 \cdot 10^{-3}$, $\beta = c_a/c_v(1 + R/r) \approx 16.4\alpha \approx 4.9 \cdot 10^{-2}$ and $\tilde{f}(x_a, x_a^\tau) = t_0^2 V_{\text{str}}/(P_0 c_a) f(x_a P_0, x_a^\tau P_0)$. Notice that $\tilde{f}$ and f share the same monotonicity and sign properties. Hence, the equilibrium of the system in equation (9) becomes

$$(x_a, x_v, x_h) = \left(1, \frac{1}{1+\frac{R}{r}}, \frac{1}{1+\frac{r}{R}}\right)$$

Linearizing equation (9) in terms of the deviation from the equilibrium $(\bar{x}_a, \bar{x}_v, \bar{x}_h)$, under assumption (4), gives

$$\begin{aligned} \dot{\bar{x}}_a &= -\bar{x}_a + \bar{x}_v + \bar{x}_h \\ \dot{\bar{x}}_v &= \alpha \bar{x}_a - \beta \bar{x}_v \\ \dot{\bar{x}}_h &= -\gamma \bar{x}_a - \delta \bar{x}_a^\tau \end{aligned} \tag{10}$$

where $\gamma = -\partial \tilde{f}/\partial x_a(1, 1)$ and $\delta = -\partial \tilde{f}/\partial x_a^\tau(1, 1)$. Notice that all the parameters here are positive, that α only depends on the ratio of the compliances, and that β depends on this ratio as well as the ratio of the resistances. In case of the example above one gets $\gamma \approx 2\beta_H$ and $\delta \approx 2\alpha_H$ assuming that $P_0 = \alpha$ (the relative error made by this assumption is less than 10%).

We now write equation (10) as

$$\dot{x} + \boldsymbol{A}x + \boldsymbol{B}x^\tau = 0 \tag{11}$$

where x and x^τ denotes the transposes of $(\bar{x}_a, \bar{x}_v, \bar{x}_h)$ and $(\bar{x}_a^\tau, \bar{x}_v^\tau, \bar{x}_h^\tau)$, respectively, and

$$\boldsymbol{A} = \begin{pmatrix} 1 & -1 & -1 \\ -\alpha & \beta & 0 \\ \gamma & 0 & 0 \end{pmatrix} \quad \text{and} \quad \boldsymbol{B} = \begin{pmatrix} 0 & 0 & 0 \\ 0 & 0 & 0 \\ \delta & 0 & 0 \end{pmatrix}$$

The associated characteristic equation is then given by

$$\Delta(\lambda, \tau) = \det(\lambda \boldsymbol{I} + \boldsymbol{A} + \boldsymbol{B}\mathrm{e}^{-\lambda\tau}) = P(\lambda) + Q(\lambda)\mathrm{e}^{-\lambda\tau} = 0 \tag{12}$$

where

$$P(\lambda) = \lambda^3 + (\beta + 1)\lambda^2 + (\gamma + \beta - \alpha)\lambda + \gamma\beta$$

and

$$Q(\lambda) = (\lambda + \beta)\delta$$

Notice that all coefficients in P and Q are positive, since $\beta > \alpha$, that P and Q are polynomials of degree 3 and 1, respectively, and that the only root, $\lambda_Q = -\beta$, in Q is negative and is not a root in P, since $P(\lambda_Q) = 2\beta(\beta - \alpha/2 + \gamma) > 2\beta(\gamma - \alpha + \delta) > 0$. Moreover, $P(0) + Q(0) = \beta(\gamma + \delta) \neq 0$. Hence one may use the method outlined in the elegant paper of Cooke and van den Driessche (1986) to investigate stability of the equilibrium. Notice first that the equilibrium is stable for vanishing time-delay, i.e. $\tau = 0$, by the Rough-Hurwitz criteria. The characteristic polynomial is

$$\lambda^3 + (\beta + 1)\lambda^2 + (\gamma + \delta + \beta - \alpha)\lambda + (\gamma + \delta)\beta$$

where all coefficients are positive and $(\beta + 1)(\gamma + \delta + \beta - \alpha) - (\gamma + \delta)\beta = \gamma + \delta + (\beta + 1)(\beta - \alpha)$ is positive. Secondly we seek positive roots y to

$$F(y) \equiv |P(iy)|^2 - |Q(iy)|^2$$

and afterward we solve equation (12) for τ using these values of y, if any. There is possibly an infinite sequence τ_n, $n = 1, 2, \ldots$, at which there may appear stability switches. Calculating $F(y)$ one gets

$$F(y) = y^6 + Ay^4 + By^2 + C$$

where

$$A = (\beta + 1)^2 - 2(\gamma + \beta - \alpha)$$
$$B = (\gamma + \beta - \alpha)^2 - 2\gamma\beta(\beta + 1) - \delta^2$$
$$C = (\gamma^2 - \delta^2)\beta^2$$

Notice that this is a polynomial of third degree $\tilde{F}(z)$ in $z = y^2$. So we are looking for positive roots of $\tilde{F}(z)$, corresponding to positive roots $y = \sqrt{z}$ of $F(y)$, and especially of interest is the number of such. The roots of $\tilde{F}(z)$ depend continuously on the four parameters $(\alpha, \beta, \gamma, \delta)$. We divide the parameter space $\boldsymbol{R}_+^4$ into regions by hypersurfaces, such that the points of each region correspond to polynomials $\tilde{F}(z)$ with the same number of positive roots. In general there are four regions, which we denote O, I, II and III corresponding to none, one, two and three positive roots, respectively. Since α and β are fairly well estimated, $\alpha = 3.0 \cdot 10^{-3}$ and $\beta = 4.9 \cdot 10^{-2}$, we will consider these

as known in the following typical scenario. Then the discussion reduces to the 2-dimensional (γ, δ)-parameter space $\boldsymbol{R}_+^2$, where the regions are separated by curves. The parameter space is divided naturally into two subspaces, $C < 0$ and $C > 0$, corresponding to $\delta > \gamma$ and $\delta < \gamma$, respectively. By Descartes' theorem it follows that the regions of one and three positive roots are located in the subspace $\delta > \gamma$, and those of none and two positive roots are located in the subspace $\delta < \gamma$. Moreover, by Descartes' theorem, three positive roots demands that $A < 0$, $B > 0$ and $C < 0$. These demands are inconsistent with the expressions for A, B and C. Therefore, there is one positive root if and only if $\delta > \gamma$. The boundary between regions O and II is characterized by that there are one non-positive root and one positive double root. Simulations show that these curves and regions are low sensitive to the exact values of α and β. However, below it is shown that the specific value of the solutions to equation (12) are indeed sensitive to the exact values of α and β. Figure 5 shows the regions for the estimated values of α and β.

5.3 Discussion of the regions

A first rough estimate for γ and δ is $\gamma = 2.34$ and $\delta = 1.67$. However, these estimates are with some uncertainty, and we may only expect that $\gamma \in [1, 6]$ and $\delta \in [1, 6]$. Hence, none of the possibilities none, one, or two positive roots can at present be excluded. Therefore we briefly sketch what happens in each of these regions:

Region O: If there are no positive roots of $\tilde{F}(z)$, the equilibria stay stable for all values of $\tau \geqq 0$, since it is stable for $\tau = 0$, and no stability switches can occur. However, the physiologically realistic range has no intersection with region O.

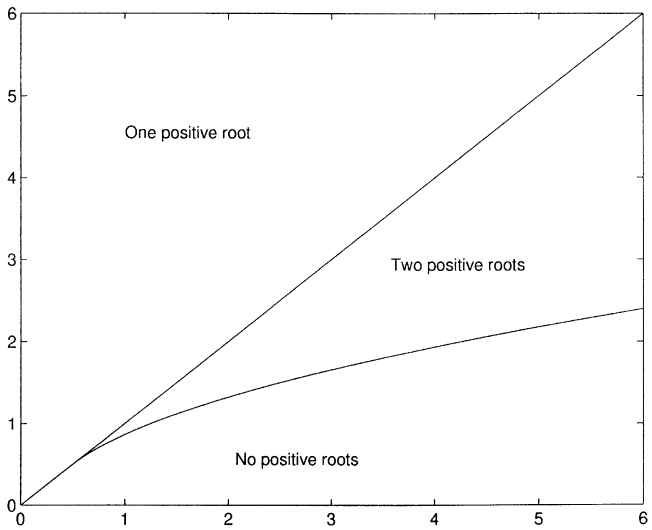

Fig. 5. The regions of different numbers of positive roots in the (γ, δ)-parameter space

Example o) $\gamma = 2.3$ and $\delta = 1.4$ In this case there are no positive roots, in fact there is only one real root of $\tilde{F}(z)$, $z = -0.024$. So in this case the equilibrium is stable for all values of $\tau \geqq 0$.

Region *I*: If there is precisely one positive simple root, say z_1, of $\tilde{F}(z)$, then there exists an infinite sequence, $\{\tau_n\}_{n=0}^{\infty}$, $\tau_n = \tau_0 + n(2\pi/y_1)$, $n \in \boldsymbol{N}$, with $y_1 = \sqrt{z_1}$, such that the pairs (y_1, τ_n) solves equation (12). When τ, considered as a parameter, runs from zero to infinity, there may appear stability switches for $\tau = \tau_n$. Since the equilibrium is stable for $\tau = 0$ it follows that it loses its stability at $\tau = \tau_0$ and stay unstable for $\tau > \tau_0$. Then there is only one stability window, $[0, \tau_0[$, in this case. Numerical considerations show that in the case of one positive simple root, $\tau_0 < 0.5$ second, for $\gamma, \delta \in [1, 6]$, as in example *i*) below. Therefore, this case seems to be excluded as physiologically realistic, since τ experimentally is estimated to be in the range one to four seconds.

Example i) $\gamma = 4.36$ and $\delta = 4.84$. In this case there is one positive root, $z_1 = 8.24$, of $\tilde{F}(z)$, corresponding to $y_1 = 2.87$. Then equation (1) gives $\tau_0 = 0.35$ seconds. So in this case the equilibrium is stable only for $\tau \in [0, 0.35[$ and unstable else. The frequency for $\tau = 0.35$ seconds is 0.3 Hz.

Region *II*: If there are precisely two positive simple roots of $\tilde{F}(z)$, say z_1 and z_2, with $z_1 > z_2$, there exist two infinite sequences $\{\tau_n^1\}_{n=0}^{\infty}$ and $\{\tau_n^2\}_{n=0}^{\infty}$, $\tau_n^1 = \tau_0^1 + n(2\pi/y_1)$ and $\tau_n^2 = \tau_0^2 + n(2\pi/y_2)$, $n \in \boldsymbol{N}$, with $y_1 = \sqrt{z_1}$ and $y_2 = \sqrt{z_2}$, such that the pairs (y_1, τ_n^1) and (y_2, τ_n^2) solve equation (12). Since $y_1 > y_2$ the equilibrium becomes unstable at $\tau = \tau_0^1$, stable again at $\tau = \tau_0^2$ (if $\tau_0^1 < \tau_0^2$), and so on, alternating between stable and unstable, until $\tau = \tau^* = \tau_n^1$ for some finite n. This is a consequence of the fact that $2\pi/y_1 < 2\pi/y_2$, so destabilising stability switches occur, on average, more frequently than stabilising stability switches. In fact, there appear

$$n^* = \left[\frac{\tau_0^1 - \tau_0^2 + \dfrac{2\pi}{y_2}}{2\pi\left(\dfrac{1}{y_2} - \dfrac{1}{y_1}\right)} \right]$$

stability windows and n^* windows of instability (here the square brackets denote the smallest integer larger than the number in the brackets). The length of the first stability window $[0, \tau_0^1[$ is τ_0^1, the length of the $(n+1)$th stability window is

$$\tau_0^1 - \tau_0^2 + \frac{2\pi}{y_1} + n \cdot 2\pi\left(\frac{1}{y_1} - \frac{1}{y_2}\right)$$

for $n = 1, 2, \ldots, n^* - 1$, and the length of the n'th window of instability is

$$\tau_0^2 - \tau_0^1 + (n-1) \cdot 2\pi\left(\frac{1}{y_2} - \frac{1}{y_1}\right)$$

for $n = 1, 2, \ldots, n^* - 1$, The last window of instability is $[\tau^*, \infty[$, where $\tau^* = \tau^1_{n^*}$. As shown in the examples below two stability windows are likely (within the physiologically parameter range $\gamma, \delta \in [1, 6]$), one with possible values of τ less than 0.5 seconds, and the other with window included in [3, 7] seconds.

Example ii) $\gamma = 5.22$ and $\delta = 4.80$. In this case there are two positive roots, $z_1 = 4.4$ and $z_2 = 84$, of $\tilde{F}(z)$, corresponding to $y_1 = 2.1$ and $y_2 = 9.2$, respectively. Then equation (12) gives $\tau^1_0 = 0.36$ and $\tau^2_0 = 7.02$ seconds. Therefore there appear two destabilising stability switches, at $\tau^1_0 = 0.36$ and at $\tau^1_1 = 3.71$ seconds, before any stabilising stability switches (the first one at $\tau^2_0 = 7.02$). So in this case there is only one stability window, $[0, 0.36[$. As in example *i*) we conclude that this case seems to be physiologically unrealistic.

Example ii') $\gamma = 5.56$ and $\delta = 4.24$. In this case there are two positive roots, $z_1 = 8.4$ and $z_2 = 1.44$, of $\tilde{F}(z)$, corresponding to $y_1 = 2.9$ and $y_2 = 1.2$, respectively. Then equation (12) gives $\tau^1_0 = 0.42$ and $\tau^2_0 = 3.7$ seconds. So in this case there are two stability windows $[0, 0.42[$ and $[3.7, 3.8[$ seconds, and two windows of instability $[0.42, 3.7[$ and $[3.8, \infty[$ seconds (qualitatively the system is equivalent to that shown in Fig. 6). The frequency is 2 Hz for $\tau = 0.42$ seconds and 5 Hz for $\tau = 3.7$ seconds. We conclude that this case is physiologically unrealistic due to the large frequency.

Example ii'') $\gamma = 2.34$ and $\delta = 1.67$. In this case there are two positive roots, $z_1 = 2.67$ and $z_2 = 1.00$, of $\tilde{F}(z)$, corresponding to $y_1 = 1.64$ and $y_2 = 1.00$, respectively. Then equation (12) gives $\tau^1_0 = 1.34$ and $\tau^2_0 = 4.00$ seconds. So in this case there are two stability windows $[0, 1.34[$ and $[4.00, 7.49[$ seconds, and two windows of instability $[1.34, 4.00[$ and $[7.49, \infty[$ seconds, see Fig. 6. The oscillation frequency for $\tau = 4.00$ seconds is 0.1 Hz. We conclude that this case seems to be physiologically realistic.

From these stability considerations we conclude that $\gamma \geqq \delta$, since otherwise we are in region I, which gives physiologically unrealistic results for $\gamma, \delta \in [1, 6]$.

5.4 Further discussion of the parameters

The solutions of the characteristic equation (12) depend on the parameters, i.e. the compliances and the resistances. It turns out that the system may be unstable (oscillatory) for some values of the time-delay τ and then becomes stable for the same time-delay by, for example, a decrease in the peripheral resistance, see Fig. 7. The reason for this is the exact location of the stability and instability windows are sensitive to the parameters. The windows move continuously with the values of the parameters.

It is known, Wesseling et al. (1982), Koepchen (1984) and Cavalcanti et al. (1995), that the mean arterial pressure is in fact not in a steady state but rather is oscillatory, approximately with a frequency of 0.1 Hz and an amplitude less

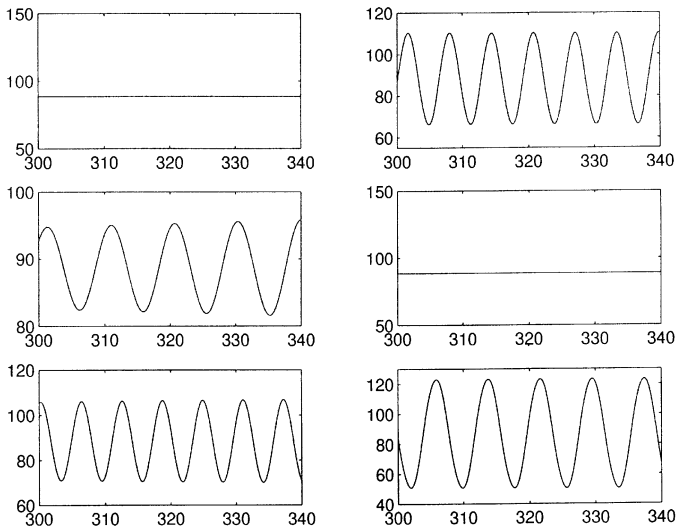

Fig. 6. The arterial pressure $P_a(t)$ in mmHg vs. time in seconds for six different values of the time-delay. Upper left: $\tau = 1.0$ seconds, upper right: $\tau = 1.4$ seconds, middle left: $\tau = 3.9$ seconds, middle right: $\tau = 5.0$ seconds, lower left: $\tau = 7.5$ seconds, lower right: $\tau = 10.0$ seconds. For $\tau = 3.9$ seconds one observe oscillations with a frequency of 0.1 Hz and an amplitude of 7 mmHg, as in the case of Mayer waves. The values of the parameters are $\alpha_H = 0.84$ seconds^{-2}, $\beta_H = 1.17$ seconds^{-2}, $\alpha_s = \alpha_p = 93$ mmHg and $\beta_s = \beta_p = 7$

than 10 mmHg. In the literature these oscillations are known as the 10 seconds Mayer waves, Seidel and Herzel (1995). In the literature it is suggested that such 10 seconds Mayer waves may be caused by the time-delay. If we demand the bifucation frequency, the frequency at the stability switches, to be 0.1 Hz (Mayer waves), then equation (12) gives

$$\delta = \frac{1}{\sin(\tau)}$$

and

$$\gamma = 1.0 - \cot(\tau)$$

From this it follows that the physiological range of τ, demanding a bifucation frequency of 0.1 Hz, is $]\pi/4, \pi[\approx]1.26, 5.03[$ seconds. For $\tau = 4$ seconds one get $\delta = 1.67$ and $\gamma = 2.34$ or correspondingly $\alpha_H \approx 0.84\,\text{sec}^{-2}$ and $\beta_H \approx 1.17\,\text{sec}^{-2}$, as were chosen as our first rough estimates. The system is oscillatory corresponding to the value of τ belonging to an instability window, see Fig. 6. However our simulations show that the oscillations are sensitive to changes in the parameters, for example the peripheral resistance. In fact, if we decrease the peripheral resistance by 20% then the oscillations may disappear, corresponding to the window of instability, which τ belongs to, moves away

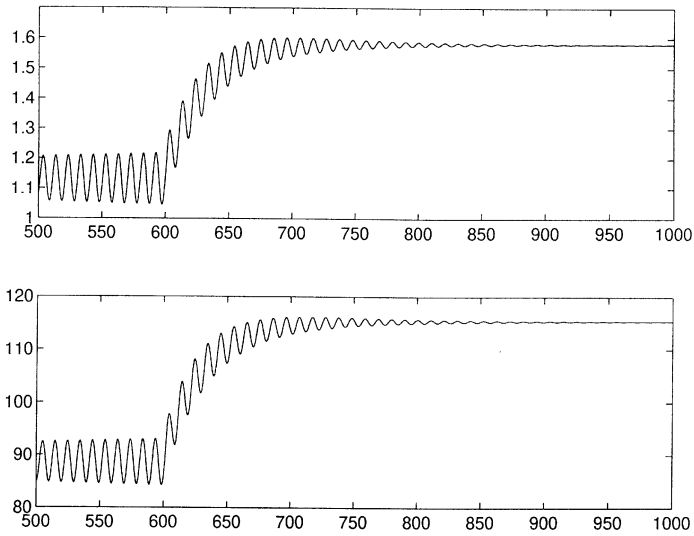

Fig. 7. Oscillations in the heart rate $H(t)$ in seconds^{-1} (upper) and in arterial pressure $P_a(t)$ in mmHg (lower), vs. time in seconds, are sensitive to the value of the peripheral resistance. At time $t = 600$ seconds the peripheral resistance decreases exponentially by 20%. Before $t = 600$ seconds one observe oscillations with a frequency of 0.1 Hz and an amplitude of 6 mmHg, as in the case of Mayer waves. After $t = 600$ seconds the oscillators vanish. The vanish of the parameters are $\alpha_H = 0.84$ seconds^{-2}, $\beta_H = 1.17$ seconds^{-2}, $\alpha_s = \alpha_p = 93$ mmHg and $\beta_s = \beta_p = 7$ and the time-delay is $\tau = 4.0$ seconds

such that τ then belongs to a window of stability, this is shown in Fig. 7. Hence we suggest an experiment which shows the sensitivity of the 10 seconds Mayer waves to the parameters, especially on the peripheral resistance. Such an experiment could determine whether or not the 10 second Mayer waves is due to time-delay.

When considering the full feedback system, including the stroke volume as a non-constant function, the coefficients A, B and C in the six order polynomial $F(y)$ become

$$A = (\beta + 1)^2 - 2(\eta\gamma + \beta - \alpha) - \xi^2$$
$$B = (\eta\gamma + \beta - \alpha)^2 - 2\eta\gamma\beta(\beta + 1) - \beta^2\xi^2 - \eta^2\delta^2$$
$$C = (\gamma^2 - \delta^2)\eta^2\beta^2$$

where η and ξ are two parameters characterizing the inotropic effect. Numerical analysis shows that there appear regions in typical planes parallel to two axis in the 4-dimensional $(\gamma, \delta, \eta, \xi)$-parameter space $\boldsymbol{R}^4_+$ similar to those described for the (γ, δ)-parameter space above (Fig. 5).

We end this section with the observation that the approximation $r = 0$ in the modelling reduces equation (1), describing the uncontrolled non-pulsatile

systemic part of the cardiovascular system, to the well-known equation from the classical Windkessel model

$$\dot{P}_a(t) = -\frac{1}{c_a R} P_a + \frac{V_{\text{str}}}{c_a} H$$

Together with the feedback mechanism described in Sect. 4 one gets an analytically more manageable system. Theorem 1 and the proof takes over, with equilibrium given by $P_a = P_o$, for some set-point value P_o, and $H = H_o = 1/(RV_{\text{str}})P_o$ (which is equation (7) in the limit $r \to 0$). Then direct calculation gives that the (γ, δ)-parameter space are divided into region quite similar to what is shown in Fig. 5. The curves dividing the regions then become $\gamma = \delta$ and the part of the parabola $\gamma = \delta^2 + 1/4$ where $\gamma > 1/2$. However, the resulting stability windows and the discussion thereof is similar to what we get without the approximation $r = 0$.

In the next section we turn to simulations and verification by use of experimental data.

6 Simulation and verification

In this section we show how the model responds to a decrease in peripheral resistance. In Kappel and Peer (1993) simulations, obtained by use of their model, were compared to data obtained in a bicycle ergometer test. Such a short term submaximal workload is assumed to affect the peripheral resistance only. Simulations show that the peripheral resistance responds to a sudden step increase in workload by decreasing exponentially with a time-constant of approximately 30 seconds. Figure 8 shows the response of the model, presented in this paper, to such a 20% decrease in peripheral resistance. The simulation obtained by use of our model agrees with the experimental data given, despite the choice of a very simple model for the uncontrolled cardiovascular system. Furthermore the venous pressure and the stroke volume behave as expected. Taking into account the large individual variation, for example due to the fitness state of the person used in the experiment, we conclude that the model provides a satisfactory description.

7 Discussion, summary and outlook

We present a direct modelling of the chronotropic and inotropic parts of the non-linear baroreflex-feedback mechanism. The modelling includes a description of both the sympathetic and parasympathetic nervous system, including time-delays. This modelling is based on physiological theory and empirical facts, to our knowledge for the first time.

The model of the feedback mechanism is evaluated on an expanded, but simple, Windkessel model of the cardiovascular system. Stability, with special

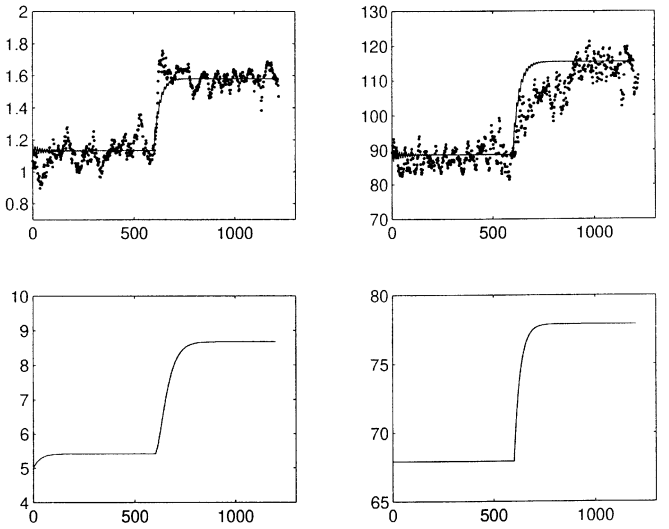

Fig. 8. How the model of the cardiovascular system responds to an exponential decrease in peripheral resistance, by 20% from 1.05 mmHg sec/ml to 0.84 mmHg sec/ml. In this simulation we have used $\tau = 5.0$ seconds only to avoid oscillations in steady state. Solid curves represent simulations and dots represent data, obtained by Kappel and Peer (1993) (with permission). Upper left shows heart rate $H(t)$ in seconds^{-1} vs. time t in seconds, upper right show arterial pressure $P_a(t)$ in mmHg vs. time t in seconds, lower left shows the venous pressure P_v in mmHg vs. time t in seconds, and lower right shows the stroke volume $V_{str}(t)$ in ml vs. time t in seconds. The parameter values are $\alpha_H = 0.84$ seconds^{-2}, $\beta_H = 1.17$ seconds^{-2}, $\alpha_s = \alpha_p = 93$ mmHg and $\beta_s = \beta_p = 7$

attention to the effect of the value of the time-delay, is analyzed. The analysis shows that it is likely that there appear several windows of stability separated by windows of instability with respect to the time-delay τ. Moreover, the exact location of these windows are sensitive to the value of the other parameters in the model. It is shown that a 20% decrease in peripheral resistance, as is likely when a person is going from rest to exercise (with a workload of approximately 50 Watt), might change the pattern and location of these stability and instability windows. Then the state of the system may change from being unstable, i.e. oscillatory, to being stable, or vice versa. At the stability switches a bifucation takes place. Near to the stability switches in one direction the system is in or approaches a stable steady state and in the opposite direction the state performs oscillations. For physiologically realistic time-delays, for example $\tau = 4$ seconds, the system performs oscillations with a frequency of 0.1 Hz and an amplitude less than 10 mmHg, as in the case of Mayer waves. However, these oscillations are sensitive to variations in the parameters, as described above. A simple clinical experiment is suggested to decide whether or not the Mayer waves originate from time-delay. Finally we simulate data obtained in a bicycle ergometer test. This data agree with simulation results

concerning the heart rate and the mean arterial pressure. Also the simulation shows the expected behavior of the venous pressure and the stroke volume.

Based on our investigation we conclude that our model of the baroreflex-feedback mechanism captures the major effect of the real physiological mechanism being modelled.

In the near future at least three aspects will be investigated. How does a limit in the work performed by the heart affect the analysis and the conclusions? How do the ignored effects of the baroreflex-feedback mechanism, e.g. the effect on the peripheral resistance and on the venous pool, influence both the model and the results? How will a pulsatile system behave when imposed for our feedback model? In fact a major point is that with our choice of approach is it possible not only to state these and other questions but also to answer them.

Acknowledgements. Finally I thank Professor F. Kappel and O. Peer for letting us use their data, obtained from ergometer bicycle tests, which we use for validation of the model.

Appendix

Below we present two lists, one of the various nominal values of the parameters used in the uncontrolled model and the other of the various nominal values of the parameters used in the feedback model. When parameters differ in value between rest phase and exercise phase the first value denote the value at the rest phase and the second value typed in brackets denote the value at the exercise phase. The values for the peripheral resistance and the stroke volume approach their value at the exercise phase asymptotically. The data given in the list of parameters used in the uncontrolled model agree with those in the literature and with physiological estimated values.

List of parameters

Nominal values of parameters in the uncontrolled model:

Arterial compliance $c_a = 1.55$ ml/mmHg
Venous compliance $c_v = 519$ ml/mmHg
Peripheral resistance $R = 1.05(0.84)$ mmHg sec/ml
Venous outflow resistance $r = 0.068$ mmHg sec/ml
Stroke volume $V_{\text{str}} = 67.9(77.9)$ ml
Typical mean heart rate $H = 1.24\,\text{sec}^{-1}$
Typical mean arterial pressure $P_0 = 100$ mmHg
Typical mean venous pressure $P_{v,0} = 7$ mmHg

Nominal values of parameters in the feedback model:

$$\alpha = \frac{c_a}{c_a} = 3 \cdot 10^{-3}$$

$$\beta = \frac{c_a}{c_v}\left(1 + \frac{R}{r}\right) = 4.9 \cdot 10^{-2}$$

$\alpha_0 = \alpha_s = \alpha_p = 93(121)\,\text{mmHg}$
$\beta_0 = \beta_s = \beta_p = 7$
$\alpha_H = 0.84\,\text{sec}^{-2}$
$\beta_H = 1.17\,\text{sec}^{-2}$
$\gamma_H = 0$

References

Allison, J., Sagawa, K., Kumada, M.: An open-loop analysis of the aortic arch barostatic reflex. Am. J. Physiol. **217**, 1576–1584 (1969)
Berger, S.: Flow in large blood vessels. Cont. Math. **141**, 479–518 (1993)
Borst, C., Karemaker, M.: Time delays in the baroreceptor reflex. J. Aut. Nerv. Syst. **9**, 399–409 (1983)
Cavalcanti, S., Belardinelli, E., Severi, S.: Numerical simulation of the short-term heart regulation. In Power, H., Hart, R. (eds.) Computer Simulations in Biomedicine, pp. 115–122. Southampton, Boston: Computational Mechanics Publications 1995
Cooke, K., van den Driessche, P.: On zeroes of some transcendental equations. Funkcialaj Ekvacioj **29**, 77–90 (1986)
El'sgol'ts, L., Norkin, S.: Introduction to the Theory and Application of Differential Equations with Deviating Arguments. New York, London: Academic Press 1973
Grodins, F.: Intergrative cardiovascular physiology: A mathematical synthesis of cardiac and blood vessel hemodynamics. Quart. Rev. Biol. **34**(2), 93–116 (1959)
Grodins, F.: Control Theory and Biological Systems. New York: Columbia University Press 1963
Guyton, A.: Textbook of Medical Physiology (Sixth ed.). Philadelphia, London, Toronto, Mexico City, Rio de Janeiro, Sydney, Tokyo: W.B. Saunders Company 1981
Guyton, A., Harris, J.: Pressoreceptor-autonomic oscillation: A probable cause of vasomoter waves. Am. J. Physiol. **165**, 158–166 (1951)
Kappel, F., Peer, R.: A mathematical model for fundamental regulation processes in the cardiovascular system. J. Math. Biol. **31**, 611–631 (1993)
Koepchen, H.: History of Studies and Concepts of Blood Pressure Waves. In Miyakawa, K., Koepchen, H., Polosa, C. (eds.) Mechanisms of Blood Pressure, pp. 3–23. Tokyo, Berlin: Japan Sci. Soc. Press/Springer-Verlag 1984
Korner, P.: Integrative neural cardiovascular control. Physiol. Rev. **51**(2), 312–367 (1971)
Lee, E., Markus, L.: Foundation of Optimal Control Theory. New York, London, Sydney: John Wiley and Sons 1967
Levy, M., Zieske, H.: Autonomic control of cardiac pacemaker. J. Appl. Physiol. **27**, 465–470 (1969)
Lighthill, J.: Mathematical Biofluiddynamics. Philadelphia: Society for Industrial and Applied Mathematics 1975
Milhorn, H.: The Application of Control Theory to Physiological Systems. Philadelphia, London: W.B. Saunders Company 1966
Noldus, E.: Optimal control aspects of left ventricular ejection dynamics. J. Theo. Biol. **63**, 275–309 (1976)
Noordergraaf, A.: Circulatory System Dynamics. New York: Academic Press 1978

Olufsen, M., Ottesen, J.: Outflow Conditions in Human Arterial Flow. In Power, H., Hart, R. (eds.) Computer Simulations in Biomedicine, pp. 249–256. Southampton, Boston: Computational Mechanics Publications 1995

Ono, K., Uozumi, T., Yoshimoto, C., Kenner, T.: The Optimal Cardiovascular Regulation of the Arterial Blood Pressure. In Kenner, T., Busse, R., Hinghofer-Szalkay (eds.) Cardiovascular System Dynamics; Model and Measurements, pp. 119–139. Plenum Press 1982

Pedley, T.: The Fluid Mechanics of Large Blood Vessels. London, New York, New Rochelle, Melbourne, Sydney: Cambridge University Press 1980

Peskin, C.: Partial Differential Equations in Biology. Lecture Notes from CIMS (Courant Institute of Mathematical Sciences), New York 1976

Rideout, V.: Mathematical and Computer Modeling of Physiological Systems. Medical Physics Publishing 1991

Russel, D.: Mathematics of Finite-Dimensional Control Systems; Theory and Design. New York, Basel: Marcel Dekker 1979

Seidel, H., Herzel, H.: Modelling Heart Rate Variability Due to Respiration and Baroreflex. In Mosekilde, E., Mouritsen, O. (eds.) Modelling the Dynamics of Biological Systems, Nonlinear Phenomena and Pattern Formation, pp. 205–229. Berlin, Heidelberg, New York: Springer-Verlag 1995

Suga, H., Sagawa, H., Kostiuk, D.: Controls of ventricular contractility assessed by pressure-volume ratio, E_{max}. Cardio. Res. **10**, 582–592 (1976)

Suga, H., Sagawa, H., Shoukas, A.: Carotid sinus baroreflex effects on instantaneous pressure-volume ratio of the canine left ventricle. J. Physiol. Soc. Japan **36**, 104–105 (1974)

Taylor, M.: Optimality Principles Applied to the Design and Control Mechanisms of the Vascular System. In The Arterial System; Dynamics, Control Theory and Regulation. pp. 181–194, Springer-Verlag 1978

Tham, R.-Y.: A Study of Effects of Halothane on Canine Cardiovascular System and Baroreceptor Control. Xerographic printed by UMI Dissertation Services, A Bell & Howell Company, 1995 (1988)

Ursino, M.: A Mathematical Model of the Interaction Between Arterial and Cardiopulmonary Baroreceptors During Acute Cardiovascular Stress. In Power, H., Hart, R. (eds.) Computer Simulations in Biomedicine, pp. 139–146. Southampton, Boston: Computational Mechanics Publications 1995

Warner, H.: The frequency-dependent nature of blood pressure regulation by carotid sinus studied with an electric analog. Circ. Res. **VI**, 35–40 (1958)

Warner, H.: Use of analogue computers in the study of control mechanisms in the circulation. Fed. Proc. **21**, 87–91 (1962)

Warner, H., Cox, A.: A mathematical model of heart rate control by sympathetic and vagus efferent information. J. Appl. Physiol. **17**, 349–358 (1962)

Warner, H., Russel, R.: Effect of combined sympathetic and vagal stimulation on heart rate in the dog. Circ. Res. **XXIV**, 567–573 (1969)

Wesseling, K. et al.: Baromodulation as the Cause of Short Term Blood Pressure Variability. In Alberi, G., Bajzer, Z., Baxa, P. (eds.) Applications of Physics to Medicine and Biology, pp. 247–276. World Scientific 1982